Vol 13 No 3, March 2004
1009-1963/2004/13(03)/0401-08

Chinese Physics

© 2004 Chin. Phys. Soc.
and IOP Publishing Ltd

Optical transitions in Er^{3+} doped lead germanate glasses*

Yang Zhong-Min(杨中民)†, Xu Shi-Qing(徐时清),
Hu Li-Li(胡丽丽), and Jiang Zhong-Hong(姜中宏)

Shanghai Institute of Optics and Fine Mechanics, Chinese Academy of Sciences, Shanghai 201800, *China*

(Received 30 June 2003; revised manuscript received 18 August 2003)

Er^{3+}- and Er^{3+}/Yb^{3+}-doped lead germanate glasses that are suitable for use in fibre lasers and optical amplifiers as well as optical waveguide devices have been fabricated and characterized. The absorption spectra from near-infrared to visible were obtained and the Judd–Ofelt parameters were determined from the absorption band. Intense and broad 1.53μm infrared fluorescence and visible upconversion luminescence were observed under 976 nm diode laser excitation. For 1.53μm emission band, the full widths at half-maximum are 36, 37, 51 nm for GPE, GPYE and GPFE samples, respectively. For frequency upconversion emission, the intense bands centred at around 524, 545, 657nm are due to the $^4S_{3/2} + {}^2H_{11/2} \rightarrow {}^4I_{15/2}$ and $^4F_{9/2} \rightarrow {}^4I_{15/2}$ transitions of Er^{3+} ions. The quadratic dependence of the green and red emissions on excitation power indicates that the two-photon absorption process occurs under the 976nm excitation.

Keywords: Judd–Ofelt theory, germanate glass, optical transition, upconversion
PACC: 7855, 4255R, 7840

1. Introduction

Over the past decades, much attention has been paid to the development of infrared and upconversion lasers and optical amplifiers. Laser emission and amplified spontaneous emission studies have been reported in crystal, bulk glasses, and optical fibres doped with rare-earth ions such as Er^{3+}, Yb^{3+}, Tm^{3+}, Pr^{3+}, and Ho^{3+} etc.[1–4] Of the doping host materials, bulk glass particularly attracts much interest because it can be drawn into a fibre and fabricated into a channel waveguide. Recently, numerous reports have been available, in which detailed spectroscopic properties of Er^{3+} were analysed in many glasses such as silicate, phosphate, borate, germanate, and fluoride glasses.[5–9] Each glass host presents certain characteristics that favour specific applications. Fluoride glass often acts as the frequency upconversion host material due to its lower phonon energy.[10,11] But few reports are available for fluoride glass acting as the amplifier host because of its poor chemical durability. Silicate glass has been investigated as the optical amplifier material because it possesses a good chemical durability and strong mechanical strength. However, it is difficult to obtain frequency upconversion emission in silicate glass due to its large phonon energy. A host glass is desirable to present mediate phonon energy to achieve the frequency upconversion and minimal absorption coefficient within the wavelength range of interest to obtain an appropriate signal gain. In particular, germanate glasses have recently been investigated because of their potential as a frequency upconversion laser material and optical amplifiers.[12–14]

In this work, lead germanate glasses have been chosen as host materials to study the spectroscopic properties of Er^{3+}. These glasses possess good chemical durability in air atmosphere, strong mechanical strength, high optical damage threshold, and good compatibility with waveguide fabrication process.[15] This glass system also has no tendency to crystallize and can be prepared at relatively low temperatures.[16] As previously reported, they are suitable for developing low loss, high strength and low cost fibres and waveguide devices.[17–20]

*Project supported by the National Natural Science Foundations of China (Grant Nos 60307004 and 60207006) and the Fund of Optical Science and Technology of Shanghai (Grant No 022261046).
† Corresponding author: E-mail: yangzm@mail.siom.ac.cn

2. Experiment

2.1. Glass composition and preparation

Three samples of Er^{3+}-doped lead germanate glasses were prepared by mixing anhydrous Pb_3O_4, PbF_2, GeO_2, and Er_2O_3 powders. The composition of the glasses expressed in mol% for the "GPE", "GPYE" and "GPFE" are as follows, respectively: (i) $60GeO_2$-40PbO-$0.3Er_2O_3$, (ii) $60GeO_2$-40PbO-$0.3Yb_2O_3$-$0.3Er_2O_3$, (iii) $60GeO_2$-30PbO-$10PbF_2$-$0.5Er_2O_3$. Pb_3O_4 and PbF_2 were of common reagent grade while GeO_2 was of 99.999% purity, and Er_2O_3 and Yb_2O_3 were of 99.99% purity. The appropriate masses of starting materials were carefully weighed and homogeneously blended in 20g batches. The mixtures were melted in alumina crucibles in a SiC- resistance electric furnace at a temperature of 1050°C and held for 10min. The melts were cast onto a stainless steel plate and then annealed at 380°C for 2h and allowed to cool to room temperature in a furnace at a rate of 5°C per hour. The annealed samples were cut using a slow speed diamond saw to dimensions of 15×20×2 mm and two big parallel faces were polished on a steel plate coated with 3000 mesh corundum for optical measurement.

2.2. Property measurements

The refractive indices of the studied glasses were measured using the Brewster angle method at two wavelengths. For samples GPE and GPYE, n_d=1.94113 and n_c=1.93158 at λ=587.6nm and λ=656.3nm, respectively. For samples GPFE, n_d=1.84422 and n_c=1.83300 at λ=587.6nm and λ=656.3nm, respectively. The refractive indices of the three samples at other wavelengths can be calculated from Sellmeier dispersion equation $n^2(\lambda)=1+\frac{S\lambda^2}{\lambda^2-\lambda_0^2}$,[21] where λ_0=130.2nm and S=0.895 for samples GPE and GPYE, λ_0=148.2nm and S=0.791 for the GPFE sample.

The density was measured using Archimedes' liquid-immersion method on an analytical balance with an accuracy of 0.0001g. The density of samples GPE and GPYE was 6.4362g/cm^3 and 6.2479g/cm^3 for sample GPFE.

Absorption spectra of the glass samples were recorded with a PERKIN-ELMER-LAMBDA 900UV/VIS/NIR spectrophotometer in the range of 380–1700nm. The fluorescence emission was dispersed using a 0.5m spectrometer, with a resolution of 0.5 nm, coupled to a photomultiplier. The signals were recorded using a digital storage oscilloscope connected to a computer. The fluorescence lifetime for the $^4I_{13/2}$ level of Er^{3+} was measured with a modulated light source from the InGaAs-photodiode (f=160kHz) and a 100MHz oscilloscope. Upconversion luminescence measurements were performed with a 976nm laser diode (2W) excitation and detected by a TRIAX550 spectrophotometer controlled by a computer.

All the measurements were taken at room temperature.

3. Results and discussions

3.1. Absorption spectra and Judd–Ofelt analysis

The absorption spectra of the studied glasses are shown in Fig.1, in which the band assignments are also indicated. For the three glasses the only differences are some changes in the relative band intensities. Absorption edges due to the glasses are all at about 380nm.

The radiative transition within $4f^n$ configuration of a rare-earth ion can be analyzed by Judd–Ofelt (J-O) approach.[22] The oscillator strength f_{cal} of an electric-dipole transition between the initial state $|(S,L)J\rangle$ and the final state $|(S',L')J\rangle$ is given by [10,23]

$$f_{cal}=\frac{8\pi^2 m_e c}{3h\overline{\lambda}(2J+1)}\times\frac{(n^2+2)^2}{9n}\times\sum_{t=2,4,6}\Omega_t|\langle(S,L)||U^{(t)}||(S',L')J'\rangle|^2, \quad (1)$$

where m is the electron mass, c the speed of light, $\overline{\lambda}$ is the mean wavelength between the two levels, n is the refractive index of the medium, h is the Planck's constant, Ω_t are J-O intensity parameters, $\langle||U^{(t)}||\rangle$ are the double-reduced matrix elements of unit tensor operators that are considered to be independent of the host matrix.

The experimental oscillator strengths can be obtained by integrating the absorbance for each band, and the relationship is [24]

$$f_{exp}=\frac{m_e c^2}{\pi e^2\overline{\lambda^2}N_0}\times\frac{2.303}{l}\int OD(\lambda)\mathrm{d}\lambda, \quad (2)$$

where e is the electron charge, N_0 is the number density of rare-earth ions, l is the sample thickness, and $OD(\lambda)$ is the optical density of absorption band associated with the transition considered.

Inasmuch as the magnetic-dipole oscillator strength exerts a considerable effect to the total radiative transition probability, one has to subtract it from the experimental oscillator strength. The magnetic-dipole contribution, $f_{\rm md}$, can be obtained from the refractive index of the glasses and the formula as reported in Ref.[10].

Table 1. Judd–Ofelt intensity parameters in Er^{3+}-doped GPE, GPYE, GPFE glasses.

Glass	Ω_2	Ω_4	Ω_6	rms* ($\times 10^{-7}$)
GPE	4.22	1.52	0.69	1.40
GPYE	4.21	1.51	0.71	1.30
GPFE	3.25	1.32	0.81	1.20

*rms represents the root-mean-square deviation.

J-O intensity parameters can be derived from the electric-dipole contributions of the experimental oscillator strengths by a least-squares fitting method. For the Er^{3+}/Yb^{3+} co-doped GPYE glass the $^4I_{15/2} \rightarrow {}^4I_{11/2}$ transition is not included in our analysis since the intense absorption of the $^2F_{5/2}$ level of Yb^{3+} is observed at the same wavelength region (900–1000nm), as shown in Fig.1. The J-O intensity parameters for glasses GPE, GPYE and GPFE are list in Table 1. It is obvious that the J-O intensity parameters are almost the same for the glasses GPE and GPYE within the uncertainty of calculation. This indicates that the addition of Yb^{3+} ions has little effect on the ligand field of Er^{3+}. Furthermore, in each glass the Ω_2 parameter is larger than the other parameters. A similar trend also was found in other glasses.[8] The magnitude of Ω_2 parameter, which bears a higher sensitivity to the chemical nature of the host, is indicative of the amount of covalent bonding, and the Ω_6 parameter is related to the rigidity of the host.[25] As compared with Ω_2 of the other glasses, as shown in Table 2,[23] chemical bonds associated with rare-earth ions in the glasses under investigation seem to be more ionic in nature due to the high concentration of PbO.

Table 2. Intensity parameters, $\Omega_t(10^{-20}\mathrm{cm}^2)$ of Er^{3+} in some glasses.

Glass	$\Omega_2/10^{-20}\mathrm{cm}^2$	$\Omega_4/10^{-20}\mathrm{cm}^2$	$\Omega_6/10^{-20}\mathrm{cm}^2$
Aluminate	5.60	1.60	0.61
Phosphate	6.65	1.52	1.11
Silicate	4.23	1.04	0.61
$PbO\text{-}Bi_2O_3\text{-}Ga_2O_3$	4.73	1.31	0.94
Fluoride	2.91	1.27	1.11

Some important radiative properties can be calculated by use of the values of Ω_t. The total spontaneous transition probability is given by [26]

$$A_{JJ'} = \frac{64\pi^4 e^2}{3h(2J+1)\overline{\lambda^3}} \times \left(\frac{n(n^2+2)^2}{9} S_{\rm ed} + n^3 S_{\rm md}\right), \qquad (3)$$

where

$$S_{\rm ed} = e^2 \sum_{t=2,4,6} \Omega_t |\langle (S,L)J||U^{(t)}||(S',L')J'\rangle|^2,$$

and

$$S_{\rm md} = \frac{e^2}{4m^2c^2} |\langle (S,L)J||L+2S||(S',L')J'\rangle|^2;$$

$A_{JJ'}$ is related to the radiative lifetime $\tau_{\rm R}$ of an excited state by

$$\tau_{\rm R} = \frac{1}{\sum_{J'} A_{JJ'}} \qquad (4)$$

and the branching ratio $\beta_{JJ'}$, corresponding to the emission from an excited level $|(S',L')J\rangle$ to $|(S,L)J\rangle$, is

$$\beta_{JJ'} = \frac{A_{JJ'}}{\sum_{J'} A_{JJ'}}. \qquad (5)$$

Tables 3 and 4 show the spontaneous transition probabilities, the branching ratios, and the calculated lifetimes of the optical transitions in Yb^{3+}/Er^{3+} co-doped GPYE and single Er^{3+}-doped GPFE glass, respectively. According to our results, the spontaneous transition rates in Yb^{3+}/Er^{3+} co-doped GPYE glass are higher than those in Er^{3+}-doped GPFE glass for most transitions. Two factors mainly contribute to these increases. First one is the large Ω_t values, particularly a larger Ω_6 value in GPYE glass than that in GPFE glass. Ω_6 is considered more affected by the overlap integrals of $4f$ and $5d$ orbits than $\Omega_2$and Ω_4.[25] The increase of Ω_6 value indicates the increase of these overlap integrals and suggests 6s electron density is smaller. The second is the refractive index n of GPYE glass which is higher than that of GPFE glass, resulting in an increase of radiative transitions. The

branching ratios for the transitions $^4S_{3/2} \rightarrow {}^4I_{15/2}$ and $^4F_{9/2} \rightarrow {}^4I_{15/2}$ in GPYE are 67% and 91%, in GPFE are 67% and 94%, respectively. Thus, it is possible to obtain efficient green and red emissions in these glasses under suitable excitation conditions.

Table 3. Predicted spontaneous radiative transition rates and lifetimes of Yb^{3+}, Er^{3+} co-doped GPYE glass.

Transitions	Energy/cm^{-1}	A_{ed}/s^{-1}*	A_{md}/s^{-1}*	β	τ_R
$^4I_{13/2} \rightarrow {}^4I_{15/2}$	6521	123.2	71.0	1	5.15
$^4I_{11/2} \rightarrow {}^4I_{15/2}$	10235	171.7		0.81	4.70
$^4I_{13/2}$	3714	20.7	20.5	0.19	
$^4I_{9/2} \rightarrow {}^4I_{15/2}$	12495	217.3		0.80	3.69
$^4I_{13/2}$	5974	49.6		0.18	
$^4I_{11/2}$	2260		4.2	0.02	
$^4F_{9/2} \rightarrow {}^4I_{15/2}$	15312	2163.6		0.91	0.42
$^4I_{13/2}$	8791	117.6		0.05	
$^4I_{11/2}$	5077	79.3		0.03	
$^4I_{9/2}$	2817	4.8		0.01	
$^4S_{3/2} \rightarrow {}^4I_{15/2}$	18365	1319.1		0.67	0.5
$^4I_{13/2}$	11844	539.6		0.27	
$^4I_{11/2}$	8310	46.4		0.02	
$^4I_{9/2}$	5870	77.5		0.04	
$^2H_{11/2} \rightarrow {}^4I_{15/2}$	19171	11376.7			
$^4F_{7/2} \rightarrow {}^4I_{15/2}$	20492	3868.2			
$^4F_{5/2} \rightarrow {}^4I_{15/2}$	22158	1589.1			

* A_{ed} and A_{md} denote the electric-dipole and magnetic-dipole transition probabilities, respectively.

Table 4. Predicted spontaneous radiative transition rates and lifetimes of the Er^{3+}-doped GPFE glass.

Transitions	Energy/cm^{-1}	A_{ed}/s^{-1}	A_{md}/s^{-1}	β	τ_R
$^4I_{13/2} \rightarrow {}^4I_{15/2}$	6528	109.8	60.2	1	5.9
$^4I_{11/2} \rightarrow {}^4I_{15/2}$	10250	147.6		0.80	5.5
$^4I_{13/2}$	3722	183.	17.5	0.20	
$^4I_{9/2} \rightarrow {}^4I_{15/2}$	12502	157.9		0.76	4.79
$^4I_{13/2}$	5974	47.2		0.226	
$^4I_{11/2}$	2252	3.6		0.014	
$^4F_{9/2} \rightarrow {}^4I_{15/2}$	15349	1717.3		0.94	0.55
$^4I_{13/2}$	8821	89.9		0.05	
$^4I_{11/2}$	5099	131.		0.007	
$^4I_{9/2}$	2847	3.2		0.003	
$^4S_{3/2} \rightarrow {}^4I_{15/2}$	18365	1269.8		0.67	0.53
$^4I_{13/2}$	11837	513.7		0.27	
$^4I_{11/2}$	8115	40.7		0.02	
$^4I_{9/2}$	5863	67.2		0.04	
$^2H_{11/2} \rightarrow {}^4I_{15/2}$	19172	7586.1			
$^4F_{7/2} \rightarrow {}^4I_{15/2}$	20492	3425.5			

3.2. Luminescence

The fluorescence spectra are shown in Fig.2. Significant enhancement for the 1.53μm infrared emission in Yb^{3+}/Er^{3+} co-doped GPYE glass can be observed. There are two factors mainly contributing to this intense emission. First, the larger spontaneous transition rates of the $^4I_{13/2}$ level in the GPE and GPYE glasses make them strongly emitting at 1.53μm. The second is the introduction of Yb^{3+} ions, which results in the increase of optical absorption of the GPYE glass at 976nm. The populations of $^4I_{11/2}$ and $^4I_{13/2}$ levels are increased because of the energy transfer between the excited $^2F_{5/2}$ state of Yb^{3+} and the $^4I_{15/2}$ ground

level of Er^{3+}. Consequently, the probability of radiative emission from the $^4I_{13/2}$ level is increased in the GPYE glass. The lifetimes of the $^4I_{13/2}$ level are 3.2, 4.2, 5.6 ms for GPE, GPYE, and GPFE glass, respectively. Within the error of determination, the quantum efficiency for the $^4I_{13/2}$ level in GPFE glass is almost 100%, while for GPE and GPYE glasses the quantum efficiencies are 62% and 82%. Such features may result from the fluorescence quenching of hydroxyl (OH) impurity in GPE and GPYE glasses. The infrared transmission spectra, shown in Fig.3, reveal that a broad absorption band of OH group in the range 2.77–3.57μm exists in the glasses GPE and GPYE. With the substitution of PbO with PbF_2 the content of OH group in GPFE glass decreases and the IR transmission rate of glass increases. During the melting process, the following reaction may occur: $PbF_2 + H_2O \rightarrow PbO + 2HF$.

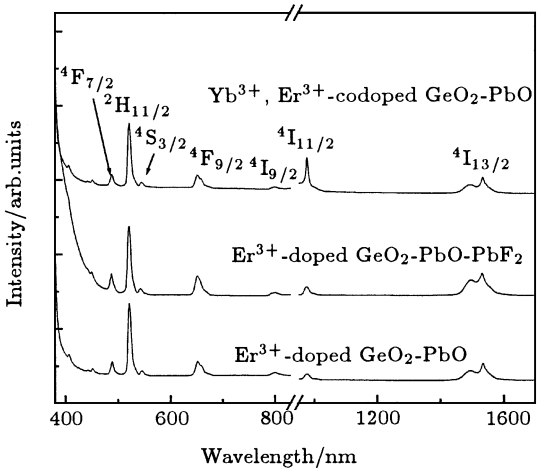


Fig.1. Absorption spectra of GPE, GPYE and GPFE glasses.

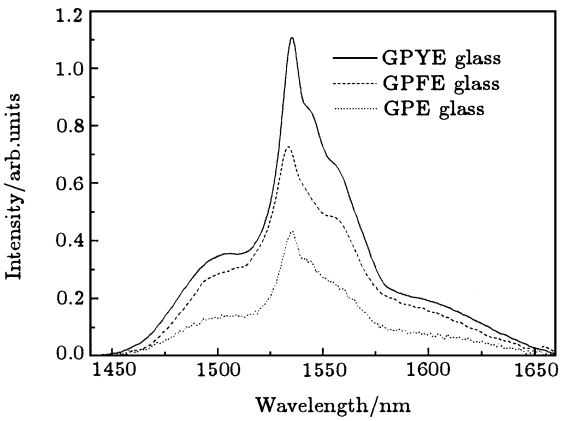


Fig.2. Infrared fluorescence spectra of GPE, GPYE and GPFE glasses excited by a 976nm diode laser.

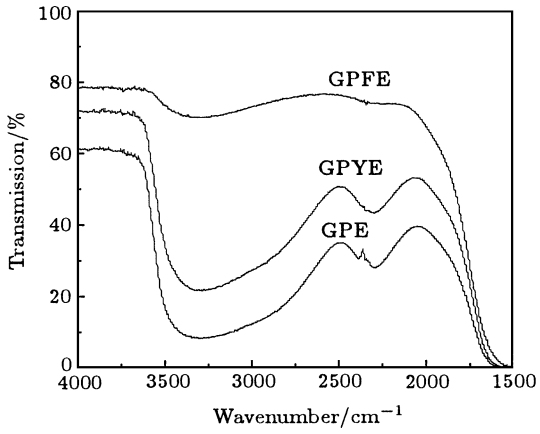


Fig.3. The IR transmission spectra of the investigated samples.

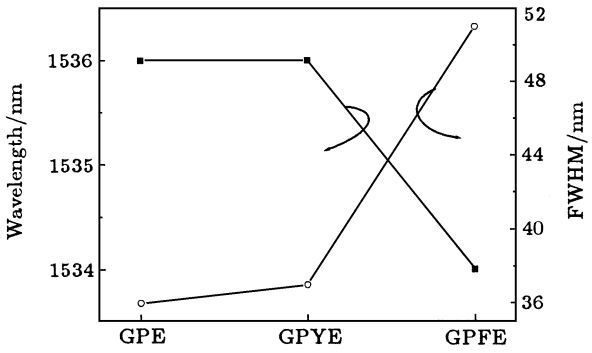


Fig.4. FWHM and peak wavelength in Er^{3+}-doped GPE, GPYE and GPFE glasses.

In different glass hosts the full width at half maximum (FWHM) of the fluorescence spectrum is often used as a semiquantitative indication to evaluate the bandwidth. Furthermore, the bandwidth is a measure of the overall extent of the stark splitting of J manifolds and is inhomogeneous due to the site-to-site variations in the local field.[25,27] Figure 4 shows the peak wavelength and FWHM of the investigated glasses. The same peak wavelength and FWHM of the fluorescence spectra in the GPE and GPYE glasses confirm that the local structure surrounding the Er^{3+} ions is almost the same in these two glasses. The larger FWHM value of the Er^{3+}-doped GPFE glass results from the mixed anion effect and the larger disorder structure at different rare-earth sites due to the addition of F^-. Fluorine ions replace oxygen ions in sites connecting lead–oxygen units, forming weak bonds and effectively depolymerizing the structure. This feature is also revealed by the calculated J-O intensity parameters. The value of Ω_2 of the GPFE glass is smaller than that of the GPYE and GPE glasses, indicating that the crystal field strength at Er sites

decreases in the GPFE glass. The reduced crystal field strength should be reflected in a decreased crystal field splitting of the J states. This is confirmed by the observation of a shift of absorption bands to shorter wavelength, as shown in Fig.4. The variation of crystal field from site to site mainly contributes to the inhomogeneous broadening of the luminescence band at 1.53μm.

3.3. Upconversion fluorescence

The visible-wavelength-range emission spectra of the Er^{3+}/Yb^{3+} co-doped GPYE glass and of the single Er^{3+}-doped GPFE glass excited by a 976nm diode laser are shown in Fig.5. In our experiments, the green and red upconversion fluorescence in sample GPYE and GPFE were easily observed but difficult to see with the naked eye in sample GPE. The green bands at 524 and 545 nm correspond to the $^4S_{3/2} \rightarrow {}^4I_{15/2}$ and $^2H_{11/2} \rightarrow {}^4I_{15/2}$ optical transitions, respectively. The red weak emission at 657nm is associated with the $^4F_{9/2} \rightarrow {}^4I_{15/2}$ transition. The stronger upconversion emission, as shown in Fig.5, in the GPFE glass arises from the low quenching effects of OH groups and the high doping concentration of Er^{3+}.

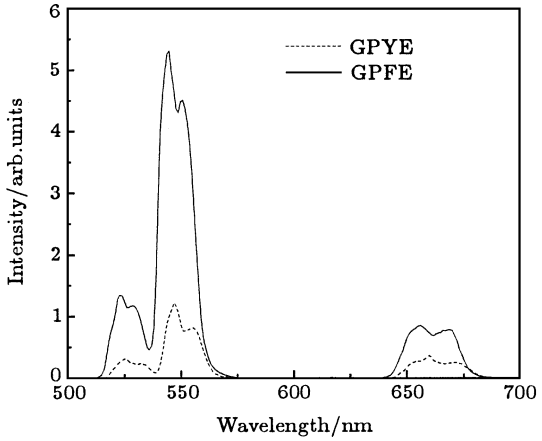


Fig.5. Upconversion spectra of Er^{3+}-doped GPFE and Er^{3+}/Yb^{3+} co-doped GPYE glasses under 976 nm excitation.

In an upconversion mechanism the upconversion emission intensity I_{UP} is proportional to the mth power of the infrared (IR) excitation intensity I_{IR}, i.e. [28]

$$I_{UP} \propto I_{IR}^m, \tag{6}$$

where m is the number of the IR photons absorbed per upconversion photon emitted. A plot of $\log I_{UP}$ versus $\log I_{IR}$ yields a straight line with slope m. Figure 6 shows such a plot for the 524, 545 and 657nm emissions in the GPFE glass, and the values of m obtained were 1.87, 1.78 and 1.86, respectively. In the GPYE glass the values of m obtained were 1.79, 1.80 and 1.80. The small fluctuation of the slope within ± 0.1 possibly results from the inhomogeneity of the glass sample or the effect of Yb^{3+} on the anti-Stokes transitions. The fact that the slope is smaller than 2 comes mainly from a saturation effect because the pump beam was focused into the sample. Similar effects due to saturation have been observed and discussed.[29] These results confirm that two photons contribute to the upconversion of the three visible emission bands.

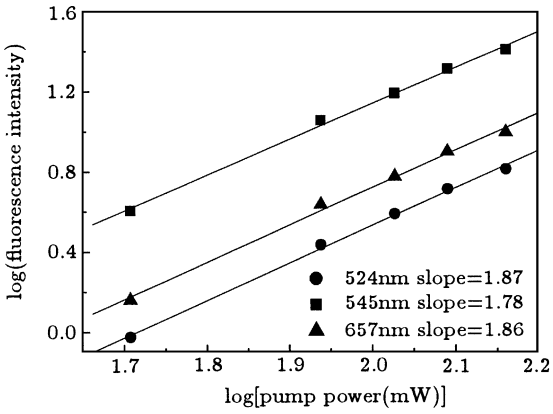


Fig.6. Dependence of upconversion emission intensity on excitation power under 976nm excitation for Er^{3+}-doped GPFE glass.

The possible upconversion mechanisms in the glasses are shown in Fig.7. When the GPFE glass is directly excited at 976nm, the energy is stored in the $^4I_{11/2}$ level. Subsequently, part of the excited energy in the $^4I_{11/2}$ level relaxes nonradiatively to the $^4I_{13/2}$ level and part of the excited $^4I_{11/2}$ Er^{3+} ions absorb a 976 nm photon to the $^4F_{7/2}$ level. The excited energy stored in the $^4F_{7/2}$ level relaxes nonradiatively to the $^2H_{11/2}$ level because of the low energy gap: for example, about 1300cm^{-1} in the GPFE glass. A fast thermal equilibrium is established between the $^2H_{11/2}$ and $^4S_{3/2}$ levels, resulting in the intense green emission.[30] In addition, the energy transfer (ET) through the $^4I_{11/2}$ level should also be considered and can be described as $2Er^{3+}(^4I_{11/2}) \rightarrow Er^{3+}(^4F_{7/2}) + Er^{3+}(^4I_{13/2})$, but its contributions are much smaller than those of the excited-state absorption (ESA) from the $^4I_{11/2}$ level due to the relatively low concentration of Er^{3+} (less than 1mol%).[31] For the red upconversion, the population of the $^4F_{9/2}$ level is the total results of ET and ESA processes from the $^4I_{13/2}$ level and a contribution from the higher energy $^4S_{3/2}$ level by nonradiative relaxation. The ET and ESA processes can be de-

scribed as $Er^{3+}(^4I_{13/2})+Er^{3+}(^4I_{11/2}) \rightarrow Er^{3+}(^4F_{9/2})+ Er^{3+}(^4I_{15/2})$ and $Er^{3+}(^4I_{13/2})$ + a photon $\rightarrow$ $Er^{3+}(^4F_{9/2})$, respectively.

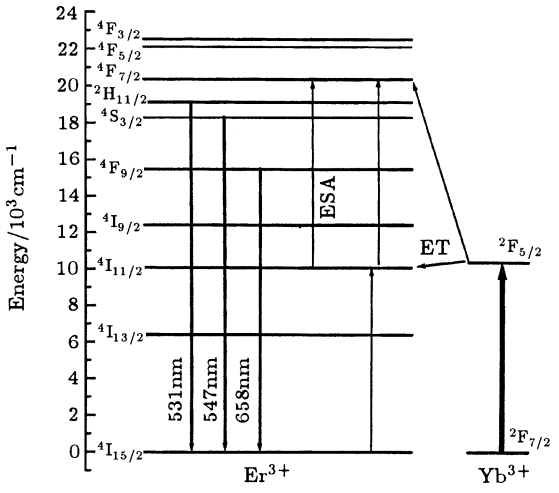


Fig.7. Simplified energy-level diagram of the Yb^{3+} and Er^{3+} ions. Upward arrows indicate excitation photons and the downward ones stand for fluorescence emission.

Figure 7 also shows the possible upconversion mechanism in the Er^{3+}/ Yb^{3+} co-doped GPYE glass. The excitation processes for 524 and 545nm green bands are as follows:

$$Er^{3+}(^4I_{15/2}) + \text{a photon} \rightarrow Er^{3+}(^4I_{11/2}); \quad (7a)$$

$$Yb^{3+}(^2F_{7/2}) + \text{a photon} \rightarrow Yb^{3+}(^2F_{5/2}); \quad (7b)$$

$$Yb^{3+}(^2F_{5/2}) + Er^{3+}(^4I_{15/2}) \rightarrow Yb^{3+}(^2F_{7/2}) + Er^{3+}(^4I_{11/2}); \quad (7c)$$

$$Yb^{3+}(^2F_{5/2}) + Er^{3+}(^4I_{11/2}) \rightarrow Yb^{3+}(^2F_{7/2}) + Er^{3+}(^4F_{7/2}); \quad (7d)$$

$$2Er^{3+}(^4I_{11/2}) \rightarrow Er^{3+}(^4F_{7/2}) + Er^{3+}(^4I_{15/2}); \quad (7e)$$

$$Er^{3+}(^4I_{11/2}) + \text{a photon} \rightarrow Er^{3+}(^4F_{7/2}). \quad (7f)$$

The population of the $^4I_{11/2}$ level increases with Yb^{3+} doped as a result of the energy transfer from Yb^{3+} ($^2F_{5/2}$) to $Er^{3+}(^4I_{11/2})$. Hence, sample GPYE should be more efficient in upconversion emission than sample GPFE. However, the OH group in the sample quenches the upconversion emission to such a great extent that we observed a weak green emission.

4. Conclusions

Er^{3+}-doped GPE and GPFE glasses and Er^{3+}/ Yb^{3+} co-doped GPYE glass have been fabricated and characterized. According to Judd–Ofelt theory we determined the J-O intensity parameters, the radiative transition rates, and the fluorescence lifetimes. Intense fluorescence at 1.53μm and efficient upconversion emissions were observed in Er^{3+}-doped GPFE glass at room temperature. In GPYE glass the relative low lifetime of the $^4I_{13/2}$ level of Er^{3+} ions and lower upconversion emission may result from the existence of OH group in the glass. The addition of PbF_2 can remove the residual OH group in the melting and increase the infrared transmission rate of the glass. The upconversion mechanisms of the GPYE and GPFE glasses and the sensitization of Yb^{3+} have been discussed. In the Er^{3+} single-doped GPFE glass, the ESA process from the $^4I_{11/2}$ level is the main factor to contribute to the intense green emission, while in the GPYE glass the ET between the $^2F_{5/2}$ level of Yb^{3+} and the$^4I_{11/2}$level of Er^{3+} and ESA from the $^4I_{11/2}$ level of Er^{3+} are both main factors.

References

[1] Laporta P, Longhi S, Taccheo and Svelto O 1993 *Opt. Commun.* **100** 311

[2] Osiac E, Sokolska I and Kuck S 2001 *J. Alloy & Comp.* **323-324** 283

[3] Balda R, Mendioroz A, Fernandez J, Arriandiaga, Griscom L S and Adam J L 2001 *Opt. Mater.* **16** 249

[4] Qiu J and Kawamoto Y 2001 *J. Fluorine Chem.* **110** 175

[5] Biswas A, Maciel G S, Kapoor R, Friend C S and Prasad P N 2003 *Appl. Phys. Lett.* **82** 2389

[6] Jiang S, Luo T, Hwang B, Smekatala F, Seneschal K, Lucas J and Peyghambarian N 2000 *J. Non-Cryst. Solids* **263/264** 364

[7] Tanabe S 1999 *J. Non-Cryst. Solids* **256/257** 282

[8] Devi A R and Jayasankar C K 1996 *J. Non-Cryst. Solids* **197** 111

[9] Osaka A, Qiu J, Miura Y and Yao T 1995 *J. Non-Cryst. Solids* **191** 339

[10] Webber M J 1967 *Phys. Rev.* **157** 262

[11] Lozano W, Araujo C B and Messaddeq Y 2002 *J. Non-Cryst. Solids* **311** 318

[12] Ribeiro S J L, Dexpert-Ghys J, Piriou B and Mastelaro V R 1993 *J. Non-Cryst. Solids* **159** 213

[13] Henderson G S and Flee t M E 1991 *J. Non-Cryst. Solids* **134** 259

[14] Lincoln J R, Mackechnie C J and Wang J 1992 *Electron. Lett.* **28** 1021

[15] Wang J, Lincoln J R and Brocklesby W S 1993 *J. Appl. Phys.* **73** 8066

[16] Lezal D, Pedlikova J and Horak J 1996 *J. Non-Cryst. Solids* **196** 178

[17] Oliveira A S, Araujo M T and Gouveia-Neto A S 1998 *J. Appl. Phys.* **83** 604

[18] Porque J, Jiang S and Hwang B 2000 *SPIE* **3942** 60

[19] MacFarlane D R, Newman P J and Plathe R 1999 *SPIE* **3849** 94

[20] Pan Z and Morgan S H 1997 *J. Lumin.* **75** 301
[21] Sarda D K, Gruber J B, Zandi B, Andrew J H and Trussell C W 2003 *J. Appl. Phys.* **93** 2041
[22] Judd B R 1962 *Phys. Rev.* **127** 750
[23] Cgoi Y G and Kim K H 1999 *J. Am. Ceram. Soc.* **82** 2762
[24] Lin H, Pun E Y B and Man S Q 2001 *J. Opt. Soc. Am.* B **18** 602
[25] Heo J, Shin Y B, Jang J N, 1995 *Appl. Opt.* **34** 4284
[26] Jacobs R R and Weber M J 1976 *IEEE J. Quantum Electron.* **QE-12** 102
[27] Yang J, Dai N, Dai S, Yang Z, Xu S, Hu L and Jiang Z 2003 *Chin. Phys.* **12** 669
[28] Yeh D C, Sibley W A, Suscavage M and Drexhage M G 1987 *J. Appl. Phys.* **62** 266
[29] Reddy B R, Nash-Stevenson S and Venkateswarlu P 1994 *J. Opt. Soc. Am.* B **11** 923
[30] Pan Z, Morgan S H, Loper A, King V, Long B H and Collins W E 1995 *J. Appl. Phys.* **77** 4688
[31] Pan Z, Morgan S H, Dyer K and Ueda A 1996 *J. Appl. Phys.* **79** 8909